

QCD, Parton Model and Altarelli-Parisi equation

Mattia Rigotti

15th December 2003

Proseminar in Theoretical Particle Physics WS 03/04
Prof. Z.Kunszt
ETH Zürich

Contents

1	Introduction	3
2	Deep inelastic scattering	4
2.1	Kinematic variables	4
2.2	Cross section and structure functions	5
2.2.1	Calculation of the leptonic tensor $L_{\mu\nu}$	5
2.2.2	The hadronic tensor $W^{\mu\nu}$	7
2.2.3	The cross section and the structure functions	7
3	The naive parton model	8
4	The parton model and QCD: violation of scaling	11
4.1	The QCD improved parton model	11
4.2	Contribution from one-gluon emission	12
4.3	Interpretation of the violation of scaling	13
5	Appendix: Calculation of $\sigma(\gamma^*q \rightarrow qg)$	14

1 Introduction

In 1969, after *Hofstadter's* first measurements of the charge distribution in the neutron that suggested a substructure of this particle, a new series of electron-proton scattering experiments performed at SLAC revealed that protons were composed of smaller objects, entities named *partons*.

This kind of experiment can be considered as a modern version of *Rutherford's* experiment, with the nucleons playing the part of the gold atoms and the partons being the corresponding of the atom's core. It was suggested that these partons were in fact *quarks*.

Quarks were already introduced in 1964 by *Murray Gell-Man* as fundamental objects in a model that explained the possibility to classify all hadrons observed so far in geometrical patterns by an underlying $SU(3)$ symmetry. In this model, the fundamental three-dimensional representations correspond to three (anti)quarks, each of them carrying a characteristic 'flavour'. The observed hadrons correspond to higher dimensional irreducible representations of $SU(3)_f$. The mesons follow a reduction of $3 \times \bar{3}$ and baryons, like the proton, form $3 \times 3 \times 3$ (three quarks).

These considerations were nothing more than group theoretical speculations, until in the late 1960s Bjorken and Feynman introduced the *parton model*. This could explain the experimental results obtained during *deep inelastic* scattering processes of electrons from protons, where the proton is shattered and a system with a large number of hadrons is produced, giving at the same time a justification of the mathematical structure of the quark model.

Bjorken and Feynman assumed the proton to be a loosely bound assemblage of a small number of constituent, called *partons*. This include quarks (and antiquarks), which are fermions carrying electric charge, and other neutral species responsible for their binding, which now we know to correspond with gluons. By assumption, these constituents are incapable of exchanging large momenta q^2 through the strong interaction. However, the quarks have the electromagnetic interactions of elementary fermions, so that an electron scattering from a quark can knock it out of the proton. The time scale of the hard scattering process is very short compared that of inter-parton interactions, hence the other partons on the proton can be regarded as spectators in the scattering process. After the collision both the proton remnant and the struck quark hadronise into 'jets'. Figure 1 shows a graphical presentation of an electron-proton collision in this Ansatz.

This model was then confirmed 1974 in the frame of QCD. In particular the assumption of weak interacting partons is a feature of the asymptotic freedom, and the hadronisation of colour confinement.

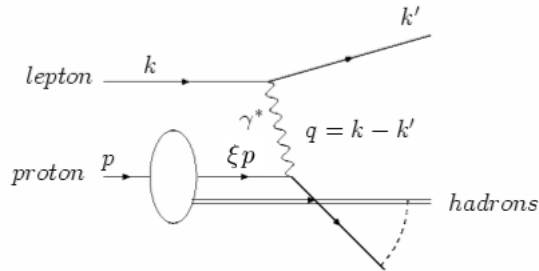


Figure 1: Kinematics of deep inelastic electron scattering in the parton model.

However not all the predictions of this so-called '*naive parton model*' are verified. In particular following this simple model in the limit of a big momentum exchange between the photon and the parton (*Bjorken limit*), $Q^2 = -q^2 \rightarrow \infty$, we would expect the structure of the target to be independent of Q^2 (*Bjorken scaling*). As we will see, this is not the case, and the broking of this scaling is still considered as one of the most powerful tests of perturbative QCD.

In the following chapters I will briefly illustrate the description of the deep inelastic scattering in the parton model. Then we will examine the relation with QCD, and at last consider a quantitative description of the scaling violation deriving the *Altarelli-Parisi equation*.

2 Deep inelastic scattering

In this section our main aim is to calculate the cross section of a deep inelastic lepton-proton scattering (see Fig. 2). We will then compare our result with the one obtained considering the parton model, that is thinking of the scattering process as happening between the lepton and a parton (see Fig. 1).

2.1 Kinematic variables

Let's consider the scattering of a high-energy lepton off a hadron target as shown in Figure 2. The four-momenta of the incoming and outgoing lepton are labelled by k^μ and k'^μ respectively, the momentum of the proton by p^μ and the momentum transfer by $q^\mu = k^\mu - k'^\mu$. The standard deep inelastic

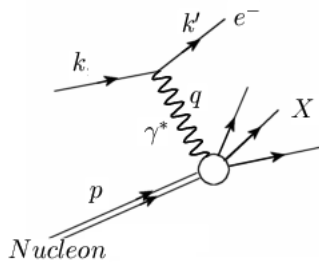


Figure 2: *Deep inelastic electron scattering, $e + p \rightarrow e + X$*

variables are defined as follows:

$$\begin{aligned}
 Q^2 &= -q^2 \\
 M^2 &= p^2 \\
 \nu &= \frac{p \cdot q}{M} = E - E' \\
 x &= \frac{Q^2}{2M\nu} = \frac{Q^2}{2M(E - E')} \\
 y &= \frac{q \cdot p}{k \cdot p} = 1 - E'/E,
 \end{aligned}$$

where the energy variables refer to the target rest frame and M is the proton mass.

2.2 Cross section and structure functions

The square of the invariant amplitude for the inelastic scattering of an electron off a hadron shown in Figure 2 averaged over spin states is given by

$$|\overline{\mathcal{M}}|^2 = \frac{e^2}{Q^4} L_{\mu\nu} W^{\mu\nu}, \quad (1)$$

where the tensor $L_{\mu\nu}$ and $W^{\mu\nu}$ describe the structure of the leptonic and hadronic vertices, respectively.

2.2.1 Calculation of the leptonic tensor $L_{\mu\nu}$

The amplitude for a virtual photon to "decay" into a e^+e^- pair as shown in Figure 3 is given by the Feynman rules by

$$A_\mu(k', s'; k, s) = -ie\bar{u}(k', s')\gamma_\mu v(k, s), \quad (2)$$

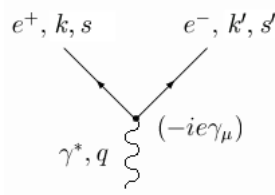


Figure 3: Amplitude for the "decay" of a virtual photon into a e^+e^- pair.

where p_i and s_i are the momenta and spins, respectively, of the outgoing spin- $\frac{1}{2}$ -fermions. If we take the absolute value squared of this amplitude and sum over final state spins we arrive at

$$\begin{aligned}
L_{\mu\nu}(k'; k) &= \frac{1}{2} \sum_{s, s'} A_\mu(k', s'; k, s) A_\nu^\dagger(k', s'; k, s) \\
&\stackrel{(2)}{=} \frac{1}{2} \sum_{s, s'} e^2 \bar{u}(k', s') \gamma_\mu v(k, s) v^\dagger(k, s) \gamma_\nu^\dagger \bar{u}(k', s') \\
&= \frac{1}{2} \sum_{s, s'} e^2 \bar{u}(k', s') \gamma_\mu v(k, s) v^\dagger(k, s) \underbrace{\gamma_\nu^\dagger \gamma_0^\dagger}_{=\gamma_0 \gamma_\nu} u(k', s') \\
&= \frac{1}{2} \sum_{s, s'} e^2 \bar{u}_a(k', s') (\gamma_\mu)_{ab} v_b(k, s) \bar{v}_c(k, s) (\gamma_\nu)_{cd} u_d(k', s') \\
&\stackrel{(*)}{=} \frac{1}{2} e^2 \not{k}'_{da} (\gamma_\mu)_{ab} \not{k}_{bc} (\gamma_\nu)_{cd} = \frac{1}{2} e^2 \text{tr}(\not{k}' \gamma_\mu \not{k} \gamma_\nu) = \frac{1}{2} e^2 \text{tr}(k'^\alpha \gamma_\alpha \gamma_\mu k^\beta \gamma_\beta \gamma_\nu) \\
&= \frac{1}{2} e^2 k'^\alpha k^\beta \underbrace{\text{tr}(\gamma_\alpha \gamma_\mu \gamma_\beta \gamma_\nu)}_{=4(g_{\alpha\mu} g_{\beta\nu} - g_{\alpha\beta} g_{\mu\nu} + g_{\alpha\nu} g_{\beta\mu})} = 2e^2 [k_\mu k'_\nu + k_\nu k'_\mu - g_{\mu\nu} k \cdot k'],
\end{aligned} \tag{3}$$

where in (*) we used the completeness relations

$$\sum_{s'} u(k', s') \bar{u}(k', s') = \not{k}' + m_e; \quad \sum_s v(k, s) \bar{v}(k, s) = \not{k} - m_e,$$

neglecting masses m_e , and the $\frac{1}{2}$ factor arises from the initial state spin averaging.

2.2.2 The hadronic tensor $W^{\mu\nu}$

The hadronic tensor contains all the information about the interaction of the electromagnetic current j_μ with the target proton P:

$$\begin{aligned} W_{\mu\nu}(p, q) &= \sum_X \langle X | j_\mu(0) | P \rangle \langle X | j_\nu(0) | P \rangle^* (2\pi)^4 \delta^{(4)}(q - p - p_X) \\ &= \sum_X \langle P | j_\nu(0)^\dagger | X \rangle \langle X | j_\mu(0) | P \rangle (2\pi)^4 \delta^{(4)}(q - p - p_X) \\ &= \int d^4z e^{iq \cdot z} \langle P | j_\nu(z)^\dagger j_\mu(0) | P \rangle. \end{aligned} \quad (4)$$

In deriving this result we have used the completeness of the final state X , *i.e.* $\sum_X |X\rangle \langle X| = 1$, and introduced an integral representation for the 4-dimensional delta function.

Current conservation requires: $\partial_\mu j^\mu = 0$, which means

$$q_\mu W^{\mu\nu} = 0, \quad q_\nu W^{\mu\nu} = 0. \quad (5)$$

Thus $W^{\mu\nu}$ has the general form

$$\begin{aligned} W^{\mu\nu}(p, q) &= -W_1(x, Q^2) \left(g^{\mu\nu} - \frac{q^\mu q^\nu}{q^2} \right) \\ &\quad + \frac{W_2(x, Q^2)}{M^2} \left(p^\mu - \frac{(p \cdot q) q^\mu}{q^2} \right) \left(p^\nu - \frac{(p \cdot q) q^\nu}{q^2} \right), \end{aligned} \quad (6)$$

where the two functions W_1 and W_2 contain the information about the structure of the hadron as 'seen' by the virtual photon. This is the most general possibility since $W^{\mu\nu}$ is a tensor which respects Eqs. (5), and which is symmetric, depending on p, q and lorentz-invariant. These last requirements in particular state that only p and q are allowed to carry the indices μ, ν .

2.2.3 The cross section and the structure functions

In the laboratory frame the initial and final electron 4-vectors are given by

$$k^\mu = \begin{pmatrix} E \\ 0 \\ 0 \\ E \end{pmatrix}, \quad k'^\mu = \begin{pmatrix} E' \\ E' \sin(\vartheta_{lab}) \\ 0 \\ E' \cos(\vartheta_{lab}) \end{pmatrix},$$

and the nucleon 4-vector is given by

$$p^\mu = \begin{pmatrix} M \\ 0 \\ 0 \\ 0 \end{pmatrix},$$

and

$$p \cdot q = M\nu.$$

The differential cross section in the laboratory frame is obtained inserting formula (3) and (6) into (1):

$$\begin{aligned} \frac{d^2\sigma}{dE'd\Omega'} &= \frac{1}{16\pi^2} \frac{E'}{E} |\overline{\mathcal{M}}|^2 = \frac{e^2}{16\pi^2 Q^4} \frac{E'}{E} L_{\mu\nu} W^{\mu\nu} \\ &= \frac{4\alpha^2 E'^2}{Q^4} \left\{ W_2(\nu, Q^2) \cos^2\left(\frac{\vartheta_{lab}}{2}\right) + 2W_1(\nu, Q^2) \sin^2\left(\frac{\vartheta_{lab}}{2}\right) \right\}, \end{aligned} \quad (7)$$

which, in the *Bjorken limit* where the proton is moving very fast ($p \gg M$), can be brought to the form

$$\begin{aligned} \frac{d^2\sigma}{dx dQ^2} &= \frac{4\pi\alpha^2}{xQ^4} (y^2 x \cdot F_1(x, Q^2) + (1-y) \cdot F_2(x, Q^2)) \quad (8) \\ &= \frac{4\pi\alpha^2}{Q^4} \left[(1 + (1-y)^2) F_1(x, Q^2) + \frac{1-y}{x} (F_2(x, Q^2) - 2xF_1(x, Q^2)) \right], \end{aligned} \quad (9)$$

where we defined the *structure functions*

$$\begin{aligned} F_1(x, Q^2) &= W_1(x, Q^2) \\ F_2(x, Q^2) &= \nu W_2(x, Q^2). \end{aligned}$$

3 The naive parton model

We again consider Fig. 1 and want to compute the scattering cross section of the reaction $e^-q \rightarrow e^-q$. Because of crossing symmetry, the matrix element for this scattering can be obtained from the corresponding matrix element for $e^+e^- \rightarrow q\bar{q}$. In fact crossing symmetry requires the amplitudes for the two processes

$$\begin{aligned} e^-(k) + q(p_q) &\rightarrow e^-(k') + q(p'_q) \\ e^+(k') + e^-(k) &\rightarrow \bar{q}(-p_q) + q(p'_q) \end{aligned}$$

to be equal. Here p_q is the momentum carried by the parton, which can be expressed as a fraction of the momentum of the proton: $p_q = \xi p$.

The amplitude for the reaction $e^+e^- \rightarrow q\bar{q}$ can be obtained by multiplying the corresponding color factor with the amplitude of $e^+e^- \rightarrow \mu^+\mu^-$, which is

a classical computation of QED. Therefore we will give here only the result in terms of our kinetic variables :

$$\frac{d\hat{\sigma}}{dQ^2} = \frac{2\pi\alpha^2 e_q^2}{Q^4} (1 + (1 - y)^2),$$

where the '^' indicates that we are considering the structure of a quark, rather than proton, target. The mass-shell constraint for the outgoing quark,

$$p_q'^2 = (p_q + q)^2 = q^2 + 2p_q \cdot q = -2p \cdot q \cdot (x - \xi) = 0,$$

implies $x = \xi$. By writing $\int_0^1 dx \delta(x - \xi) = 1$, we obtain the double differential cross section for the quark scattering process:

$$\frac{d\hat{\sigma}}{dx dQ^2} = \frac{4\pi\alpha^2}{Q^4} (1 + (1 - y)^2) \frac{1}{2} e_q^2 \delta(x - \xi). \quad (10)$$

By comparing Eqs. (10) and (8) we see that the structure functions in this simple model are:

$$\hat{F}_2 = x e_q^2 \delta(x - \xi) = 2x \hat{F}_1 \quad (11)$$

This represents a quark with an exact momentum fraction $x = \xi$.

Now we want to consider the so-called '*naive parton model*', which assumes the proton to be composed of quarks with the following characteristics:

- $q(\xi)d\xi$ represents the probability that a quark q carries a momentum fraction between ξ and $\xi + d\xi$, where $0 \leq \xi \leq 1$,
- the virtual photon scatters incoherently off the quark constituents.

In this case the proton structure functions are obtained by weighting the quark structure functions with the probability distribution $q(\xi)$,

$$\begin{aligned} F_2(x) &= 2xF_1(x) = \sum_{q,\bar{q}} \int_0^1 d\xi q(\xi) x e_q^2 \delta(x - \xi) \\ &= \sum_{q,\bar{q}} e_q^2 x q(x). \end{aligned} \quad (12)$$

The first identity, $F_2(x) = 2xF_1(x)$, is known as the *Callan-Gross relation* and is a direct consequence of the spin- $\frac{1}{2}$ nature of the quarks. The function $q(x)$ is known as the parton distribution function.

The second identity is the one which interests us the most: it predicts that the cross section only depends on one variable, the *scaling variable* x . This property is called *Bjorken scaling*. Approximate scaling is observed in the data at $x \approx 0.1$, but violation of scaling is observed for lower and higher x . Figure 4 shows F_2 versus Q^2 measured by various HERA- and fixed target experiments.

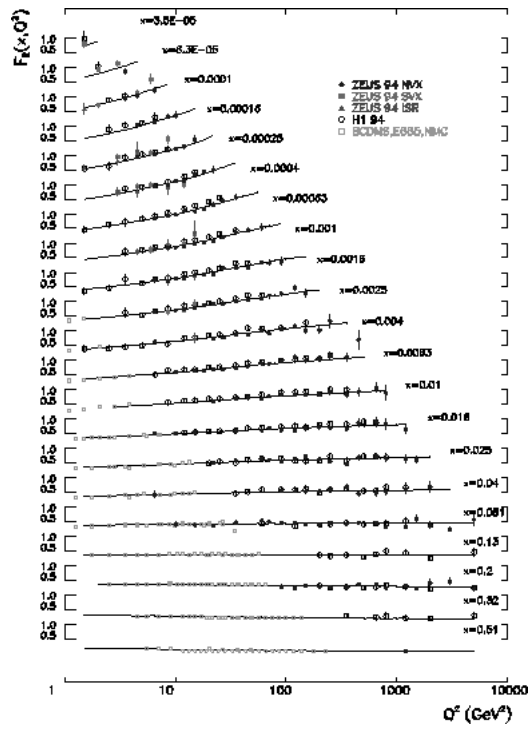


Figure 4: *The structure function F_2 measured by ZEUS, H1 and various fixed target experiments plotted against Q^2 . Bjorken scaling is observed at high x , but is gradually broken towards low x . The line represents a QCD based fit to the data.*

4 The parton model and QCD: violation of scaling

In the 'naive' parton model the structure functions *scale*, *i.e.* $F(x, Q^2) \rightarrow F(x)$ in the asymptotic (Bjorken) limit: $Q^2 \rightarrow \infty$, x fixed. In QCD, this scaling is *broken* by logarithms of Q^2 (see Fig. 4). The key point is that the parton's transverse momentum is *not* restricted to be small. In fact a quark can emit a gluon and acquire large transverse momentum k_T . QCD extends the naive quark parton model by allowing interactions between the partons via the exchange of gluons.

In this section I will calculate the structure function of a quark which can emit a gluon, *i.e.* the $O(\alpha_S)$ correction to the parton model result $\hat{F}_2 = e_q^2 x \delta(x - \xi)$ obtained in the previous section.

4.1 The QCD improved parton model

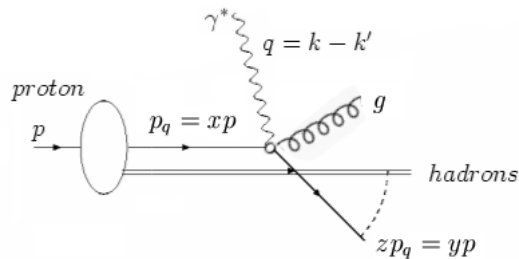


Figure 5: *Virtual photon quark total cross section, $\gamma^* q \rightarrow qg$*

A proton cannot be calculated completely in the perturbative approach. An essential ingredient in the QCD description of the proton is the concept of factorization: it is assumed that the differential cross section for the photon-proton scattering can be written as the product of a parton density and a hard scattering process:

$$d\sigma = q(x) dx \frac{d\hat{\sigma}}{dz} dz, \quad (13)$$

where as before and as indicated in Figure 5:

$q(x)$ is the probability of finding a quark with momentum $p_q = xp$,
 $\frac{d\hat{\sigma}(z, Q^2)}{dz}$ is the cross section for scattering with a value of $z = \frac{y}{x}$.

We can now integrate eq. (13) and sum over all quarks to obtain

$$\sigma(y, Q^2) = \sum_{q, \bar{q}} \int_y^1 dx q\left(\frac{y}{x}\right) \hat{\sigma}(x, Q^2), \quad (14)$$

where the limit of integration comes from the condition that $z \leq 1$.

We want to express Eq. (14) in terms of the corresponding structure functions F_2

$$F_2(x, Q^2) = \sum_{q, \bar{q}} \int_x^1 d\xi q\left(\frac{x}{\xi}\right) \hat{F}_2(\xi, Q^2). \quad (15)$$

4.2 Contribution from one-gluon emission

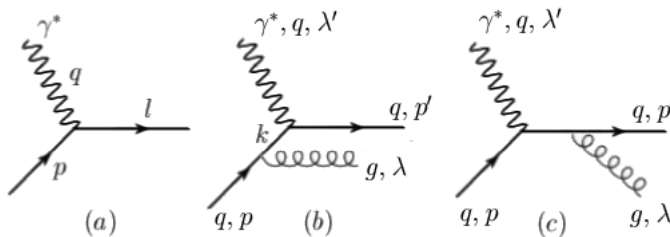


Figure 6: *Feynman diagrams for the calculation of the amplitudes for deep inelastic scattering off a quark*

Summing over all the real gluon emission diagrams contributing to the deep inelastic scattering (figure 6), together with the leading-order diagram (see the Appendix for the full derivation), give a structure function

$$\hat{F}_2(x, Q^2) = e_q^2 x \left[\delta(1-x) + \frac{\alpha_s}{2\pi} \left(P(x) \ln \frac{Q^2}{\kappa^2} + C(x) \right) \right]. \quad (16)$$

In order to obtain a proton structure function we must convolute the quark structure function \hat{F}_2 of Eq. (17) with a 'bare' distribution q_0 of a quark in a proton and sum over quark flavours, as we did before for the naive parton model, and as indicated by the factorization theorem expressed with Eq. (15). This gives

$$F_2(x, Q^2) = x \sum_{q, \bar{q}} e_q^2 \left[q_0(x) + \frac{\alpha_s}{2\pi} \int_x^1 \frac{d\xi}{\xi} q_0(\xi) \left(P\left(\frac{x}{\xi}\right) \ln \frac{Q^2}{\kappa^2} + C\left(\frac{x}{\xi}\right) \right) + \dots \right]. \quad (17)$$

Exactly as for the renormalization of the coupling constant, we can regard $q_0(x)$ as an unmeasurable, *bare* distribution. The collinear singularities are absorbed into this bare distribution at a 'factorization scale' μ , which plays a similar role to the renormalization scale. In other words, we define a 'renormalized' distribution $q(x, \mu^2)$ by

$$q(x, \mu^2) = q_0(x) + \frac{\alpha_s}{2\pi} \int_x^1 \frac{d\xi}{\xi} q_0(\xi) \left(P\left(\frac{x}{\xi}\right) \ln \frac{Q^2}{\kappa^2} + C\left(\frac{x}{\xi}\right) \right) + \dots,$$

in terms of which

$$F_2(x, Q^2) = x \sum_{q, \bar{q}} e_q^2 \int_x^1 \frac{d\xi}{\xi} q(\xi, \mu^2) \left[\delta\left(1 - \frac{x}{\xi}\right) + \frac{\alpha_s}{2\pi} P\left(\frac{x}{\xi}\right) \ln \frac{Q^2}{\kappa^2} + \dots \right]. \quad (18)$$

Taking the $\ln(\mu^2)$ partial derivative of Eq. (18) we obtain

$$\ln(\mu^2) \frac{\partial}{\partial \ln(\mu^2)} q(x, \mu^2) = \frac{\alpha_s(\mu^2)}{2\pi} \int_x^1 \frac{d\xi}{\xi} P\left(\frac{x}{\xi}\right) q(x, \mu^2).$$

This equation - known as the (Dokshitzer)-Gribov-Lipatov-Altarelli-Parisi (GLAP) equation - is the analogue of the β function equation describing the variation of $\alpha_s(\mu^2)$ with μ^2 and is one of the most important equations of perturbative QCD.

4.3 Interpretation of the violation of scaling

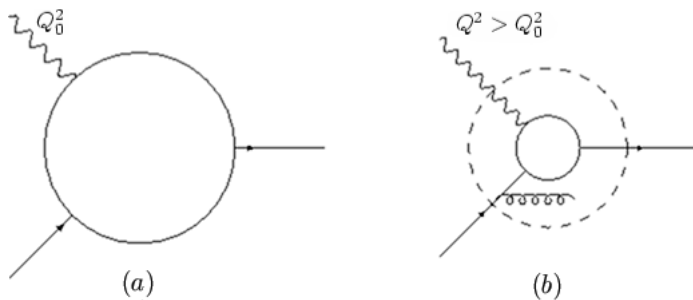


Figure 7: *With increasing Q^2 finer structure is observed*

The processes that generate the parton interactions to first order in α_s are gluon radiation ($q \rightarrow qg$), gluon splitting ($g \rightarrow gg$) and quark pair production ($g \rightarrow q\bar{q}$). The violation of Bjorken scaling observed in the data is naturally

described by these processes: a photon interacting with a quark at a certain Q_0^2 probes the proton with a finite resolution proportional to $1/Q_0^2$. If the photon probes the same quark at a higher Q^2 , the quark might have radiated a gluon not visible at Q_0^2 and the photon effectively interacts with a quark carrying less momentum (figure 7). The result is a dependence of the cross section on Q^2 .

The effect of all interactions is described by so called splitting functions, in leading order $P_{qq}(\frac{y}{x})$, $P_{gq}(\frac{y}{x})$, $P_{gg}(\frac{y}{x})$ and $P_{qg}(\frac{y}{x})$ (figure 8). Each function $P_{p'p}(\frac{y}{x})$ represents the probability that a parton of type p radiates a quark or gluon and becomes a parton of type p' carrying fraction $\frac{y}{x}$ of the momentum of parton p . Splitting functions have been calculated from perturbative QCD.

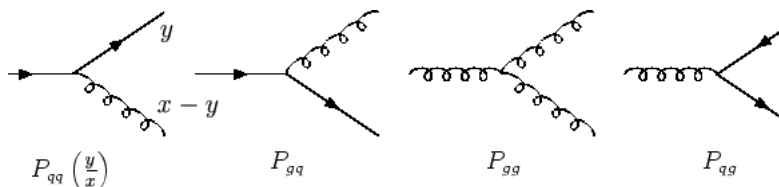


Figure 8: The processes related to the lowest order QCD splitting functions. Each splitting function $P_{p'p}(\frac{y}{x})$ gives the probability that a parton of type p converts into a parton of type p' , carrying a fraction $\frac{y}{x}$ of the momentum of parton p .

5 Appendix: Calculation of $\sigma(\gamma^* q \rightarrow qg)$

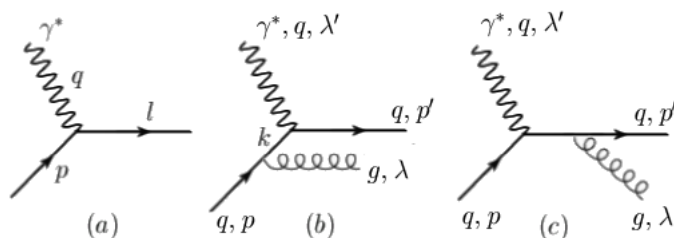


Figure 9: Feynman diagrams for the calculation of the amplitudes for deep inelastic scattering off a quark

This process has the amplitude $\mathcal{M}_1 + \mathcal{M}_2$ with (see Fig. 9)

$$\begin{aligned}\mathcal{M}_1 &= i\bar{u}(p', s')\varepsilon\mu(\lambda)(-ig_s\gamma^\mu T_{ij}^a)i\frac{\not{p}+\not{q}}{(p+q)^2}(-iee_q\gamma^\nu)\varepsilon_\nu(\lambda')u(p, s) \\ \mathcal{M}_2 &= i\bar{u}(p', s')\varepsilon\tau(\lambda)(-iee_q\gamma^\tau)i\frac{\not{p}-\not{q}}{(p-q)^2}(-ig_s\gamma^\sigma T_{ij}^a)\varepsilon_\sigma(\lambda')u(p, s)\end{aligned}$$

This gives for $|\mathcal{M}_1|^2$:

$$\begin{aligned}|\mathcal{M}_1|^2 &= \frac{g_s^2 e^2 e_q^2}{(p+q)^4} T_{ij}^a T_{ji}^a \sum_{s, s', \lambda, \lambda'} (\bar{u}(p', s')\varepsilon\mu(\lambda)\gamma^\mu)(\not{p}+\not{q})\gamma^\nu\varepsilon_\nu(\lambda')u(p, s) \\ &\quad (\bar{u}(p, s)\varepsilon^*\nu(\lambda')\gamma^\nu)(\not{p}+\not{q})\gamma^\mu\varepsilon_\mu^*(\lambda)u(p', s') \\ &= \frac{g_s^2 e^2 e_q^2}{(p+q)^4} \text{tr}(T^a T^a) \text{tr}(\not{p}'\gamma_\mu(\not{p}+\not{q})\gamma_\nu\not{p}\gamma^\nu(\not{p}+\not{q})\gamma^\mu) \\ &= \frac{64g_s^2 e^2 e_q^2}{s^2} (2(p'p + p'q)(pq) - (p'p)(2pq + q^2)).\end{aligned}$$

We use the Mandelstam-Variables

$$s = (p+q)^2, \quad t = (q-p')^2, \quad u = (p-p')^2,$$

with the properties:

$$pp' = \frac{-1}{2}u, \quad pq = \frac{1}{2}(s - q^2), \quad p'q = \frac{-1}{2}(t - q^2), \quad s + t + u = q^2,$$

and obtain

$$\begin{aligned}|\mathcal{M}_1|^2 &= \frac{32g_s^2 e^2 e_q^2}{s^2} ((-u - t + q^2)(s - q^2) + us) = \frac{32g_s^2 e^2 e_q^2}{s^2} (s(-t - u) + us) \\ &= 32g_s^2 e^2 e_q^2 \left(\frac{-t}{s}\right).\end{aligned}$$

In analogy with this result we can calculate

$$|\mathcal{M}_2|^2 = 32g_s^2 e^2 e_q^2 \left(\frac{-s}{t}\right)$$

and

$$\mathcal{M}_1\mathcal{M}_2^* = 64g_s^2 e^2 e_q^2 \left(\frac{-uq^2}{st}\right).$$

For the square of the total amplitude averaged over spins we can therefore write

$$|\overline{\mathcal{M}}|^2 = \frac{1}{12} (|\mathcal{M}_1|^2 + |\mathcal{M}_2|^2 + 2\mathcal{M}_1\mathcal{M}_2^*) = \frac{128\pi^2}{3} \alpha_s \alpha_e^2 \left(-\frac{t}{s} - \frac{s}{t} + \frac{2uQ^2}{st} \right).$$

With this result we can write the differential cross section for the subprocess $\gamma^*q \rightarrow qg$, which is given by

$$\frac{d\hat{\sigma}}{dt}(s, t) = \frac{z^2}{16\pi Q^4} |\overline{\mathcal{M}}|^2 = \frac{\pi \alpha_s \alpha_e^2 z^2}{Q^4} \frac{16}{3} \left(-\frac{t}{s} - \frac{s}{t} + \frac{2Q^2(s+t+Q^2)}{st} \right). \quad (19)$$

The total virtual photon quark cross section is arrived at by integrating Eq. (19) over t . Namely,

$$\hat{\sigma}(s) = \int_{t_{max}}^{t_{min}} \frac{d\hat{\sigma}}{dt}(s, t) dt,$$

where $t_{min} = 0$, and $t_{max} = -(s + Q^2) = -Q^2/z$.

This integral is divergent and we cannot proceed without choosing a regularization scheme. Notice that the singularity arises when the gluon is emitted parallel to the quark, and for this reason is called a collinear divergence. The key to understanding what is happening is to realize that the limit $t \rightarrow 0$ corresponds to a long-range ('soft') part of the strong interaction which is not calculable in perturbation theory.

To regularize the singularity we will change the limit of integration to $t_{min} = -\frac{m_g^2 z Q^2}{Q^2(1-z)}$, and this corresponds to giving a fictitious mass $q_g^2 = m_g^2$ to the gluon (see MG Regularization Scheme). With

$$\left(\frac{s^2 + sQ^2(s+Q^2)}{s} \right) \int_{-Q^2/z}^{-m_g^2 z Q^2 / (Q^2(1-z))} \left(-\frac{dt}{t} \right) = \frac{Q^2(1+z^2)}{z(1-z)} \ln \left(\frac{Q^2(1-z)}{m_g^2 z^2} \right),$$

we obtain

$$\hat{\sigma}(z, Q^2) = \frac{4\pi \alpha_s \alpha_e^2}{Q^2} z \left(P_{gq}(z) \ln \left(\frac{Q^2}{m_g^2} \right) + C(z) \right),$$

where we defined the *splitting function*

$$P_{gq}(z) = \frac{4}{3} \frac{1+z^2}{1-z}.$$

$\hat{\sigma}(z, Q^2)$ is proportional to the structure function F_2 :

$$\hat{F}_2(z, Q^2) = e_q^2 z \left[\frac{\alpha_s}{2\pi} \left(P(z) \ln \frac{Q^2}{\kappa^2} + C(z) \right) \right],$$

which is exactly the correction to the parton model result to obtain Eq. (17).